Research Article **Open Access**

Yifan Hao, Xuejun Zhao, Xuedan Song, Hongjiang Li, Xiaobing Zhu, and Ce Hao*

The Interaction between Graphene and Oxygen **Atom**

DOI 10.1515/phys-2016-0075 Received Apr 23, 2016; accepted May 24, 2016

Abstract: Based on the density function theory (DFT) method, the interaction between the graphene and oxygen atom is simulated by the B3LYP functional with the 6-31G basis set. Due to the symmetry of graphene ($C_{54}H_{18}$, D_{6h}), a representative patch is put forward to represent the whole graphene to simplify the description. The representative patch on the surface is considered to gain the potential energy surface (PES). By the calculation of the PES, four possible stable isomers of the C₅₄H₁₈-O radical can be obtained. Meanwhile, the structures and energies of the four possible stable isomers, are further investigated thermodynamically, kinetically, and chemically. According to the transition states, the possible reaction mechanism between the graphene and oxygen atom is given.

Keywords: Graphene; Density functional theory; Potential energy surface; Radical regioisomers; Representative patch

PACS: 31.50.Bc

Panjin 124221, China

1 Introduction

Since being discovered in 2004 [1], graphene, as the first truly two-dimensional crystal, with large surface area, high chemical stability, flexibility, superior electric and thermal conductivity [2–5], has drawn dramatic attention for use in such areas as sensors, energy conversion, photodetectors, and aerospace [6–10]. Graphene oxide (GO) as a significant raw material of mass-production graphene

Email: haoce@dlut.edu.cn; Tel./fax: +86 411 84986335

Engineering, Texas Tech University, Lubbock, TX 79404

*Corresponding Author: Ce Hao: State Key Laboratory of Fine Chemicals, Dalian University of Technology, Panjin 124221, China; Yifan Hao: State Key Laboratory of Fine Chemicals, Dalian University of Technology, Panjin 124221, China; Deptment of Chemical Xuejun Zhao, Xuedan Song, Hongjiang Li, Xiaobing Zhu: State Key Laboratory of Fine Chemicals, Dalian University of Technology,

via reduction, is an important carbon nanomaterial in the graphene family [11–14]. Because GO is rich for oxygencontaining groups in the structure, and the ratio of sp² to sp³ hybridized carbon atoms is easy to control, GO possesses brilliant performance in electronics, optics, energy conversion, environmental science, and biotechnology. It is reported that GO nanoplatelets were self-assembled to form carbon films with tunable porous morphologies and mechanical flexibility, which incorporated good electrical properties [15]. Yeh and his co-workers used GO in the photocatalytic of H₂ evolution activity. According to the Mott-Schottky equation, the results of electrochemical analysis showed that H₂ could be generated stably from the pure water or methanol solution through the GO films under mercury vapor light irradiation, even under the condition of lack of cocatalyst Pt [16]. Meanwhile, compared with other benchmark material, i.e. C60, G0 exhibits a good performance on the optical power limiting. In order to investigate optical power limiting behaviors of GO, Jiang et al. [17] prepared GO films on the plastic substrates and glass, which shows excellent broadband optical limiting. Besides, compounded GO, with other materials, can enhance the thermodynamic properties of the material [18–20]. In addition, graphene quantum dots (GQDs) as an emerging fluorescent nanomaterial, with excellent optical performance [21], easy to surface modify [22], high chemical stability [23–26], low toxicity, and good bio-compatibility [27, 28], have drawn dramatic attention in the scientific community. All in all, GO as well as GQDs have dramatically grabbed the attention of the scientific community due to their brilliant performances. Due to most of them being prepared by oxidation, it is of vital importance to understand the interaction between the graphene and oxygen atom.

In this paper, a systematic study of the interaction between the graphene ($C_{54}H_{18}$, D_{6h}) and oxygen atom is performed by the density function theory. Based on the symmetry, a representative patch is put forward to represent the whole graphene ($C_{54}H_{18}$, D_{6h}) to simplify the description. By the single point energy scan on the entire surface of the graphene, the PES between the graphene (C₅₄H₁₈, D_{6h}) and oxygen atom was obtained. Meanwhile, all the possible isomers, as well as all the TSs, were obtained to explain the possible reaction mechanism.

2 Computational details

In this study, $C_{54}H_{18}(D_{6h})$ is chosen as the whole system. Based on the symmetry of graphene, a representative patch is put forward to represent this whole graphene $(C_{54}H_{18}, D_{6h})$ to simplify the description. In calculation, we adopted the B3LYP hybrid functional with the Gaussian09 program [29-31]. The STO-3G [32], as well as the standard 6-31G(d) [33], were set as the basis sets. Firstly, graphene (C₅₄H₁₈, D_{6h}) and its corresponding symmetry group, as the initial geometries are optimized with the basis set of B3LYP/6-31G (d). Secondly, in terms of the calculation of the single point energy, the potential energy curve and the PES were obtained at the basic level of STO-3G. When calculating PES, we just need to consider the energy distribution in the whole graphene ($C_{54}H_{18}$, D_{6h}). So, the basis set of STO-3G can satisfy our requirements according to our experience. Thirdly, the isomers of C₅₄H₁₈-O on the representative patch were optimized respectively at the standard 6-31G (d). In addition, the harmonic vibrational frequency was analyzed to make sure that the stationary points at the same basis set, were real.

3 Results and discussion

3.1 The representative patch

Based on the symmetry, we chose a triangular section of the graphene $(C_{54}H_{18}, D_{6h})$ as a representative patch to make it more simple(as shown in Fig. 1). All the key points have their own symmetry. For instance, the key point of R_1 is C_{6v} symmetry; the key points of R_n (n = 2, 3, 4), b_n (n = 1, 3, 4), b_n 3, 4, 5, 6), C3, C4 are $C_{2\nu}$ symmetry; the key points of b_n (n = 1, 2, 7, 8) C1, C2 are C_s symmetry. The area of the total surface is equal to 24 and the representative patch is the 1/24. When calculated to the representative patch, it can contain the whole surface of the graphene ($C_{54}H_{18}$, D_{6h}). Hence, we just need to calculate the smallest structure unit (the patch DEF) to replace the entire graphene. On the representative patch, there are eighteen key points including four six-membered rings' centres (key points of R_1 , R_2 , R_3 , R_4), eight bond centres (key points of b_1 , b_2 , b_3 , b_4 , b_5 , b_6 , b_7 , b_8), six carbon atoms. Because the graphene ($C_{54}H_{18}$, D_{6h}) edge is saturated with hydrogenation, we just need to

take the four carbon atom (key points of C1, C2, C3, C4) into account.

To make the potential energy surface at a reasonable interaction distance between the graphene and oxygen atom, the potential energy curves of the representative patch at the different key points were discussed by the scanning of the single point energy. Fig. 2 is the potential energy curves of the representative patch, and it can be seen that two different trends are shown from the curves. The top curves show a relatively sharp trend, which belongs to the oxygen atom moving away from the bond centre of b_1 and b_2 . Meanwhile, the bottom curves have poten-

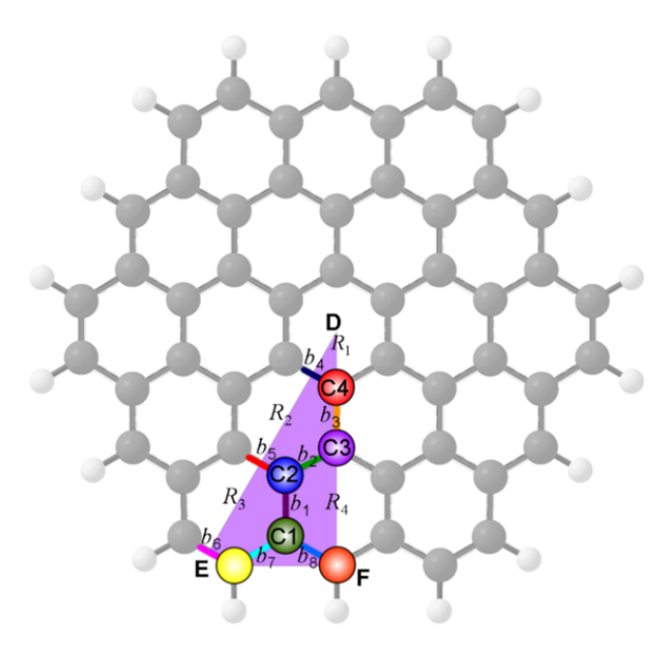


Figure 1: The representative patch of graphene ($C_{54}H_{18}$, D_{6h}).

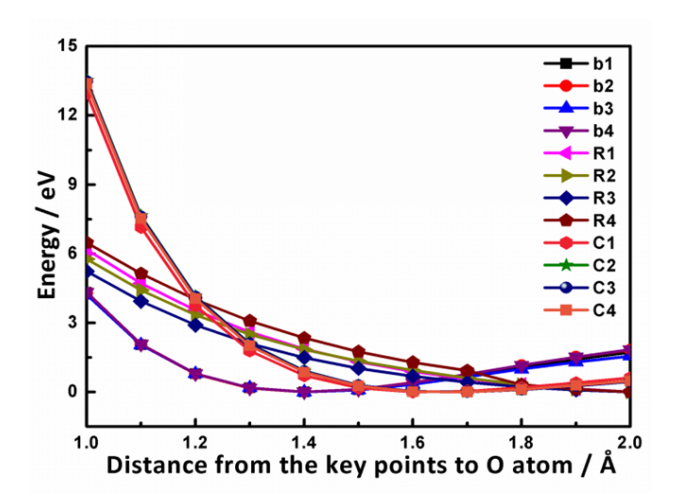


Figure 2: The potential energy curves of the representative patch as function of the height from oxygen atom to the key points.

| Structure | C-C(Å) | C-O (Å) | C-O (Å) | C-O-C(°) | Gap Energy(eV) | Rel Energ(eV) |
|--------------------|--------|---------|---------|----------|----------------|---------------|
| $C_{54}H_{18}-O^1$ | 1.546 | 1.531 | 1.510 | 61.11 | 2.433 | 0.155 |
| $C_{54}H_{18}-O^2$ | 1.521 | 1.520 | 1.522 | 60.01 | 2.728 | 0.000 |
| $C_{54}H_{18}-O^3$ | 1.540 | 1.520 | 1.513 | 61.03 | 1.932 | 0.345 |
| $C_{54}H_{18}-O^4$ | 1.516 | 1.524 | 1.524 | 59.65 | 2.449 | 0.003 |

Table 1: Geometric parameters, HOMO-LUMO gap energies and relative energies of $C_{54}H_{18}$ -O.

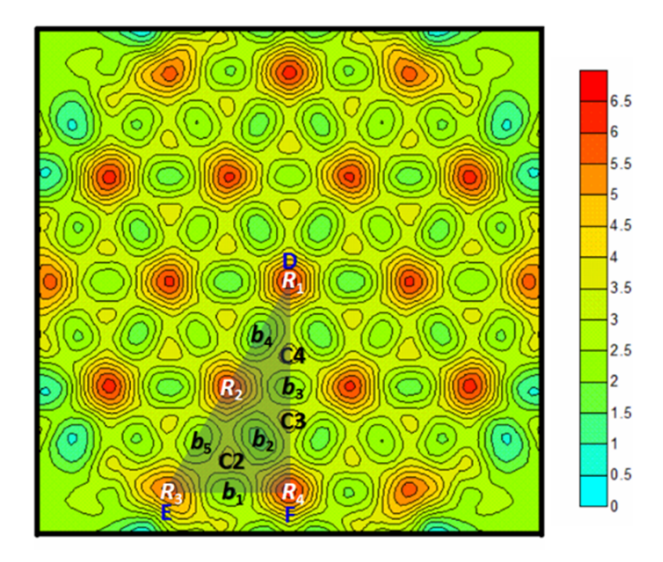


Figure 3: The potential energy surface of $C_{54}H_{18}$ -O.

tial wells, the height of which is about 1.4 Å. It expressed that there is a stable chemical adsorption site at the bond centre of the b_3 and b_4 when the oxygen atom moved away from the graphene at the normal directions.

According to the potential energy curves of the $C_{54}H_{18}$ -O radical, the potential energy surfaces were scanned at the height of 1.4 Å, as shown in Fig. 3. From the representative patch, it can be clearly observed that the key points of b_1 , b_2 , b_3 , b_4 are the minimum value of the potential energy in the wells, and the key points of R_1 , R_2 , R_3 , and R_4 are the maximum value of the potential energy. Therefore, four possible isomers are proposed theoretically, which are named $C_{54}H_{18}$ -O¹、 $C_{54}H_{18}$ -O²、 $C_{54}H_{18}$ -O³、 $C_{54}H_{18}$ -O⁴ corresponding to the bond centre of b_n (n = 1, 2, 3, 4).

3.2 The thermodynamic stability

Table 1 is the geometric parameters, HOMO-LUMO gap energies, and relative energies for the four possible isomers of $C_{54}H_{18}$ -O. However, the balanced distance of the C-O bond (including the bonds of C-O and C-O) is 1.52 Å and the mean angel of C-O-C is 60.64° .

Among the different isomers of $C_{54}H_{18}$ -O, it can be noted that $C_{54}H_{18}$ -O² is the lowest energy in total, so we set it as the zero point of the relative energy. Then $C_{54}H_{18}$ -O⁴ is only higher by 0.003 eV than $C_{54}H_{18}$ -O², which is the second most stable. And $C_{54}H_{18}$ -O³ possesses the highest energy, which is the least stable. Based on the above analysis, the ordering of thermodynamic stability is received for $C_{54}H_{18}$ -O² > $C_{54}H_{18}$ -O⁴ > $C_{54}H_{18}$ -O¹ > $C_{54}H_{18}$ -O³.

3.3 The chemical reaction activity

The HOMO–LUMO energy gap sequence enable us to describe the chemical reaction activity of the four $C_{54}H_{18}{\cdot}O$ isomers, which can also be shown in Table 1. Comparing with the HOMO–LUMO energy gaps, we can get that $C_{54}H_{18}{\cdot}O^2$ is the highest gap energy at 2.728 eV, and the $C_{54}H_{18}{\cdot}O^3$ is the lowest gap energy at 1.932 eV. According to the gap energy of HOMO–LUMO, the sequence of the chemical reaction activity is $C_{54}H_{18}{\cdot}O^2 > C_{54}H_{18}{\cdot}O^4 > C_{54}H_{18}{\cdot}O^1 > C_{54}H_{18}{\cdot}O^3$, which is consistent with the sequence of the thermodynamic stability.

3.4 The kinetics activity

TSs between different $C_{54}H_{18}$ -O radicals are calculated at the 6-31G (d) level. The results show that each TS only has one single imaginary frequency. TS1 represents the transition state of $C_{54}H_{18}$ -O¹ and $C_{54}H_{18}$ -O², and the value of single imaginary frequency is 522.24 i cm⁻¹. TS2 represents the transition state of $C_{54}H_{18}$ -O² and $C_{54}H_{18}$ -O³ with the only imaginary frequency value of 517.55 i cm⁻¹. TS3 represents the transition state of $C_{54}H_{18}$ -O³ and $C_{54}H_{18}$ -O⁴ and the value of single imaginary frequency is 439.86 i cm⁻¹.

Table 2 is the activation energies (E_a) as well as the relative energy of transition states (TS1, TS2, TS3). It shows that the E_a value of the oxygen atom to be transferred from the isomer of $C_{54}H_{18}$ - O^1 to the isomer of $C_{54}H_{18}$ - O^2 is 0.747 eV. On the reverse reaction path, the E_a value of the oxygen atom to be transferred from the isomer of $C_{54}H_{18}$ - O^2 to the isomer of $C_{54}H_{18}$ - O^1 is 0.902 eV. Another reac-

Table 2: The calculated energies and activation energy (E_a) for radical isomers $C_{54}H_{18}$ -O on the representative patch at B3LYP/6-31G (d) level

| | C ₅₄ H ₁₈ -O ¹ | TS1 | $C_{54}H_{18}-O^2$ | TS2 | C ₅₄ H ₁₈ -O ³ | TS3 | C ₅₄ H ₁₈ -O ⁴ |
|---------------|---|-------|--------------------|-------|---|-------|---|
| <i>E</i> (eV) | 0.155 | 0.902 | 0 | 1.048 | 0.345 | 0.949 | 0.003 |
| E_a (eV) | 0.747 | 0.902 | 1.048 | 0.703 | 0.604 | 0.946 | |

tion path for the isomer of $C_{54}H_{18}$ - O^2 is the oxygen atom to be transferred from the isomer of $C_{54}H_{18}$ - O^2 to the isomer of $C_{54}H_{18}$ - O^3 , the E_a value of which is 1.048 eV. So the minimum E_a value of the isomer $C_{54}H_{18}$ - O^2 is 0.902 eV. In addition, the E_a value of $C_{54}H_{18}$ - O^3 (including the isomer of $C_{54}H_{18}$ - O^3 to the isomer of $C_{54}H_{18}$ - O^2 and the isomer of $C_{54}H_{18}$ - O^3 to the isomer of $C_{54}H_{18}$ - O^4) is 0.703 eV and 0.604 eV. Thus, the minimum E_a value of the isomer $C_{54}H_{18}$ - O^3 is 0.604 eV. Meanwhile, the E_a value of the oxygen atom to be transferred from the isomer of $C_{54}H_{18}$ - O^4 to the isomer of $C_{54}H_{18}$ - O^3 is 0.946 eV. Therefore, the stability order of the kinetics activity is $C_{54}H_{18}$ - O^4 > $C_{54}H_{18}$ - O^2 > $C_{54}H_{18}$ - O^3 for the four isomers of $C_{54}H_{18}$ -O. This is a little different to the sequence of the thermodynamic stability and the chemical reaction activity.

4 Conclusions

According to the PES gained by the scanning of the single point energy, four possible isomers of $C_{54}H_{18}$ -O on the representative patch are optimized by the density functional theory method. In short, the oxygen atom is easy to absorb above the bond to form the epoxy. $C_{54}H_{18}$ -O² is the most stable isomer, calculated by analyzing the the thermodynamics and chemical reaction activity. $C_{54}H_{18}$ -O⁴ is the most stable isomer as calculated by analyzing the kinetics activity of radicals. Furthermore, investigation of the interaction between the oxygen atom and graphene is also crucial to further understanding the details of the GO and GQDs.

Acknowledgement: The financial support of the National Natural Science Foundation of China (Grant Nos. 21373042), the Fundamental Research Funds for the Central Universities of China (Grant No. DUT15RC(4)11) and Liaoning Provincial Doctor Startup Foundation of China (Grant No. 20141019). And the Project Sponsored by the Scientific Research Foundation for the Returned Overseas Chinese Scholars, State Education Ministry is greatly appreciated.

References

- Novoselov K.S., Geim A.K., Morozov S.V., Jiang D., Zhang Y., Dubonos S.V., et al., Electric field effect in atomically thin carbon films, Science, 2004, 306, 666-669.
- [2] Geim A.K., Novoselov K.S., The rise of graphene, Nat. Mater., 2007, 6, 183-191.
- [3] Shahil K.M.F., Balandin A.A., Thermal properties of graphene and multilayer graphene: applications in thermal interface materials, Solid State Commun., 2012, 152, 1331-1340.
- [4] Stoller M.D., Park S., Zhu Y., An J., Ruoff R.S., Graphene-based ultracapacitors, Nano Lett., 2008, 8, 3498-3502.
- [5] Zhu Y., Murali S., Stoller M.D., Ganesh K.J., Cai W., Ferreira P.J., et al., Carbon-based supercapacitors produced by activation of graphene, Science, 2011, 332, 1537-1541.
- [6] Bandurin D.A., Torre I., Kumar R.K., Shalom M.B., Tomadin A., Principi A., et al., Negative local resistance caused by viscous electron backflow in graphene, Science, 2016, 351, 1055-1058.
- [7] Anguita J.V., Ahmad M., Haq S., Allam J., Silva S.R P., Ultra-broadband light trapping using nanotextured decoupled graphene multilayersal, Sci. Adv., 2016, 2, e1501238.
- [8] Katsnelson M.I., Graphene: carbon in two dimensions, Mater. Today, 2007, 10, 20-27.
- [9] Zhang M.X., Zhao G.J., Modification of n-type organic semiconductor performance of perylene diimides by substitution in different positions: two-dimensional pi-stacking and hydrogen bonding, ChemSusChem, 2012, 5, 879-887.
- [10] Neto A.H.C., Guinea F., Peres N.M.R., Novoselov K.S., Geim A.K., The electronic properties of graphene, Rev. Mod. Phys., 2009, 81, 109-162.
- [11] Wei Z., Wang D., Kim S., Kim S.Y., Hu Y., Yakes M.K., et al., Nanoscale tunable reduction of graphene oxide for graphene electronics, Science, 2010, 328, 1373-1376.
- [12] Li H., Song Z., Zhang X., Huang Y., Li S., Mao Y., et al., Ultrathin, molecular-sieving graphene oxide membranes for selective hydrogen separation, Science, 2013, 342, 95-98.
- [13] Binggeli M., Christoph R., Hintermann H.E., Colchero J., Marti O., Friction force measurements on potential controlled graphite in an electrolyte environment, Nanotechnology, 1993, 4, 59-63.
- [14] Nair R.R., Wu H.A., Jayaram P.N., Grigorieva I.V., Geim A.K., Unimpeded permeation of water through helium-leak-tight graphene-based membranes, Science, 2012, 335, 442-444.
- [15] Lee S.H., Kim H.W., Hwang J.O., Lee W.J., Kwon J., Bielawski C.W., et al., Three-dimensional self-assembly of graphene oxide platelets into mechanically flexible macroporous carbon films, Angew. Chem., 2010, 122, 10282–10286.
- [16] Yeh T.F., Syu J.M., Cheng C., Chang T.H., Teng H., Graphite oxide as a photocatalyst for hydrogen production from water, Adv. Funct. Mater., 2010, 20, 2255–2262.
- [17] Jiang X.F., Polavarapu L., Neo S.T., Venkatesan T., Xu Q.H.,

Y. Hao et al.

- Graphene oxides as tunable broadband nonlinear optical materials for femtosecond laser pulses, J. Phys. Chem. Lett., 2012, 3, 785–790.
- [18] Zhao S., Li Y., Yin H., Liu Z., Luan E., Zhao F., et al., Three-dimensional graphene/Pt nanoparticle composites as free-standing anode for enhancing performance of microbial fuel cells, Sci. Adv., 2015, 1, e1500372.
- [19] Stankovich S., Dikin D.A., Dommett G.H.B., Kohlhaas K.M., Zimney E.J., Stach E.A., et al., Graphene-based composite materials, Nature, 2006, 442, 282-286.
- [20] Dikin D.A., Stankovich S., Zimney E.J., Piner R.D., Dommett G.H.B., Evmenenko G., et al., Preparation and characterization of graphene oxide paper, Nature, 2007, 448, 457-460.
- [21] Zhu S., Meng Q., Wang L., Zhang J., Song Y., Jin H., et al., Highly photoluminescent carbon dots for multicolor patterning, sensors, and bioimaging, Chem. Int. Ed., 2013, 52, 3953-3957.
- [22] Sun Y.P., Zhou B., Lin Y., Wang W., Fernando K.A.S., Pathak P., et al., Quantum-sized carbon dots for bright and colorful photoluminescence, J. Am. Chem. Soc., 2006, 128, 7756-7757.
- [23] Pei S., Zhang J., Gao M., Wu D., Yang Y., Liu R., A facile hydrothermal approach towards photoluminescent carbon dots from amino acids, J. Colloid Interface Sci., 2015, 439, 129-133.
- [24] Kong B., Zhu A., Ding C., Zhao X., Li B., Tian Y., Carbon Dot-Based Inorganic-organic nanosystem for two-photon imaging and biosensing of pH variation in living cells and tissues, Adv. Mater., 2012, 24, 5844-5848.
- [25] Han B., Wang W., Wu H., Fang F., Wang N., Zhang X., Polyethyleneimine modified fluorescent carbon dots and their application in cell labeling, Colloids Surf. B, 2012, 100, 209-214.

- [26] Ruan S., Zhu B., Zhang H., Chen J., Shen S., Qian J., et al., A simple one-step method for preparation of fluorescent carbon nanospheres and the potential application in cell organelles imaging, J. Colloid. Interface Sci., 2014, 422, 25-29.
- [27] Yang S.T., Wang X., Wang H., Lu F., Luo P.G., Cao L., et al., Carbon dots as nontoxic and high-performance fluorescence imaging agents, J. Phys. Chem. C, 2009, 113, 18110-18114.
- [28] Ge S., Ge L., Yan M., Song X., Yu J., Liu S., A disposable immunosensor device for point-of-care test of tumor marker based on copper-mediated amplification, Biosens. Bioelectron., 2013, 43, 425-431.
- [29] Becke A.D., Density-functional thermochemistry. III. The role of exact exchange, J. Chem. Phys., 1993, 98, 5648-5652.
- [30] Frisch M.J., Trucks G.W., Schlegel H.B., Scuseria G.E., Robb M.A., Cheeseman J.R., et al., Gaussian 09, revision A.01, Inc., Wallingford CT, 2009.
- [31] Lee C., Yang W., Parr R.G., Development of the colle-salvetti correlation-energy formula into a functional of the electron density, Phys. Rev. B, 1988, 37, 785–789.
- [32] Pietro W.J., Hehre W.J., Molecular orbital theory of the properties of inorganic and organometallic compounds. 3. STO-3G basis sets for first- and second-row transition metals, J. Comput. Chem., 1983, 4, 241-251.
- [33] Hehre W.J., Ditchfield R., Pople J.A., Self-consistent molecular orbital methods. XII. Further extensions of gaussian-type basis sets for use in molecular orbital studies of organic molecules, J. Chem. Phys., 1972, 56, 2257-2261.